

Accepted Manuscript

A 2D Parallel Diffusive Wave Model for floodplain inundation with variable time step (P-DWave)

J. Leandro, A.S. Chen, A. Schumann

PII: S0022-1694(14)00384-9

DOI: <http://dx.doi.org/10.1016/j.jhydrol.2014.05.020>

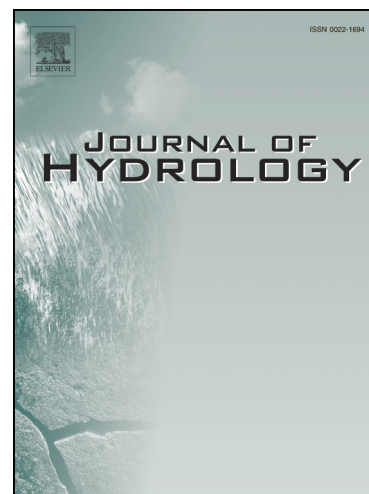
Reference: HYDROL 19619

To appear in: *Journal of Hydrology*

Received Date: 14 March 2014

Revised Date: 22 April 2014

Accepted Date: 5 May 2014



Please cite this article as: Leandro, J., Chen, A.S., Schumann, A., A 2D Parallel Diffusive Wave Model for floodplain inundation with variable time step (P-DWave), *Journal of Hydrology* (2014), doi: <http://dx.doi.org/10.1016/j.jhydrol.2014.05.020>

This is a PDF file of an unedited manuscript that has been accepted for publication. As a service to our customers we are providing this early version of the manuscript. The manuscript will undergo copyediting, typesetting, and review of the resulting proof before it is published in its final form. Please note that during the production process errors may be discovered which could affect the content, and all legal disclaimers that apply to the journal pertain.

1 **A 2D Parallel Diffusive Wave Model for floodplain inundation with variable time step (P-DWave)**

2 Leandro J. ^{1,3}, Chen, A. S. ², and Schumann, A. ¹

3 ¹ Institute of Hydrology, Water Management and Environmental Techniques, Ruhr-University

4 Bochum, Germany. E-mail: Jorge.leandro@ruhr-uni-bochum.de, Andreas.Schumann@ruhr-uni-

5 bochum.de

6 ² Centre for Water Systems, College of Engineering, Mathematics and Physical Sciences, University of

7 Exeter, UK. E-mail: a.s.chen@exeter.ac.uk

8 ³ IMAR, Department of Civil Engineering , University of Coimbra, R. Luís Reis Santos, Polo 2, 3030-788

9 Coimbra, Portugal.

10 **Abstract**

11 Growing advances in remote sensing technologies together with the widespread availability of

12 Digital terrain models (DTM) have intensified the research into two-dimensional (2D) models.

13 Supported by detailed DTM, 2D models can become very accurate tools yet not without an added

14 cost on the computational effort. Floodplain inundation is characterized by a slow varying

15 phenomenon which can last hours, days or even weeks. In this paper we aim to develop a specific

16 parallel diffusive wave model with variable time step suitable for flood inundation. Taking advantage

17 of up to 12 processors, speed-up times ranging from 1.7 to 5.2 and 1.2 to 1.7 are achieved with the

18 Matlab parallel computing toolbox and Fortran OpenMP Application Programming, respectively. The

19 variable time method and the process devised to represent Wet-Dry fronts kept the solution stable

20 and preserved absolute mass conservation. P-DWave performed well against known analytical

21 solutions and dynamic and diffusive models in a total of seven tests.

22 **Keywords:** parallelization, diffusive wave model, Wet-Dry fronts, variable time step, absolute mass

23 conservation

24 **1. Introduction**

25 The growing advances in remote sensing technologies led to the widespread use and development
26 of two-dimensional (2D) inundation models (Bradbrook *et al.*, 2013). Digital terrain models (DTM)
27 obtained from light detection and ranging (LiDAR) data enable large areas of terrain to be precisely
28 characterised, therefore rendering almost unlimited accuracy possibilities in numerical modelling.
29 Unpleasantly, the use of high resolution grids (i.e. 10 m or less) for large areas can lead to
30 unacceptable run times for 2D Models simulations, while simultaneously demanding a more
31 complex treatment of the model flow resistance (Dottori *et al.*, 2013). This can nonetheless be
32 improved by coarsening the DTM's resolution with penalty on the accuracy of the results. Herein we
33 aim to develop a 2D Parallel Diffusive Wave Model (P-DWave) with variable time step to improve the
34 computational efficiency of 2D diffusive wave models.

35 Except for catastrophic scenarios of dam break where the full dynamic equations must be applied,
36 flooding over plain areas (often termed inundation) is characterized by a slow moving phenomena
37 whereby the inundation can be modelled by the diffusive equations (Chen *et al.*, 2005). The diffusive
38 wave simplification neglects the inertial terms allowing, therefore, a simplified set of equations to be
39 solved. In general terms using a simplified set of equations leads to faster computational times,
40 however, due to stability criterion some authors have verified that at coarser resolutions (10m or
41 more) diffusive models were computationally less effective than dynamic models (Hunter *et al.*,
42 2008; and Neal *et al.*, 2012). In urban areas, Maksimovic and Prodanović (2001) suggest values
43 between 1 and 2m and Mark *et al.* (2004) between 1 and 5m as optimal grid sizes to capture all the
44 main topographic features.

45 Improvements on model performance have been the focus of recent research, particularly for
46 explicit 2D diffusive wave models (2D DWM) it has been driven by two main reasons: the higher
47 performance gain by explicit models because they use smaller time steps than their implicit
48 counterparts due to stability considerations (Hirsch, 2007), and the fact that dynamic models require

49 more complex numerical schemes than diffusive models (Prestininzi, 2008). Dottori & Todini (2011)
50 enhanced the model performance of a 2D DWM by including an inertial formulation to compute
51 discharges developed by Bates et al. (2010) and an adaptive time step developed by Zhang et al.
52 (1994). Hunter et al. (2005) upgraded the raster-based cell model LISPFLOOD-FP using an adaptive
53 time step (Bates and Roo, 2000). Liang and Borthwick (2009) improved a 2D full dynamic model by
54 using dynamically adaptive grids. Burger and Rauch (2012) implemented a parallel version of the
55 open-source implicit 1D full dynamic EPA SWMM model (Rossman, 2005). Despite published
56 improvements (Chen *et al.*, 2012), the original overland flow models such as the explicit 2D DWM
57 LISPFLOOD-FP and SIRIPLAN have proven their usefulness particular for calibration purposes (Di
58 Baldassarre *et al.*, 2009; and Horritt, 2006) or modelling of large scale sites (da Paz *et al.*, 2013).

59 If a meaningful cross-comparison of model's accuracy should use similar benchmark cases (Pender
60 and Néelz, 2010), a meaningful cross-comparison of model performance by parallelization of
61 algorithms ideally should use the same programming language and computational architecture as
62 these may affect the overall performance. Judi et al. (2011) described reductions in computational
63 time due to desktop parallelization varying from 14 to 300 times using a 16 core-processors
64 computer while Ceyhan et al. (2007) reported 1.3 to 2 times for the same number of core-
65 processors. Apart from the different languages and speed of processors used, computer acceleration
66 times are limited by Amdahl's law i.e. the speedup is limited by the time needed for the sequential
67 part of the program. It is thus clear that the former extraordinary increase was not only due to the
68 parallelization but also due to changes in the algorithm (as rightfully acknowledged by the Authors).

69 Yu (2010) and Neal et al. (2009) reported speedups in line with Amdahl's law ranging from 1.6 to 1.8
70 and from 3.4 to 5.2 using 2 and 8 core-processors respectively.

71 In this paper we develop a parallelized diffusive wave (P-DWave) model with an adaptive time step.
72 The aim is to develop an accurate flood inundation model whose efficiency can be scalable through
73 the use of multi-processor computer architecture. The Model is developed in MatlabTM and

74 Fortran™ languages and tested in an AMD Opteron™ Processor 6276 with 12 cores 2.3GHz CPU and
 75 192GB of RAM available at the RUHR University of Bochum. Next section describes the Parallel
 76 Diffusive Wave Model (P-DWave)

77 2. Parallel Diffusive Wave Model (P-DWave)

78 2.1. The Diffusive Wave Model Equations

79 The 2D Shallow Water Equations (SWE) can be written in the conservative form as:

$$\frac{dh}{dt} + \nabla(\mathbf{u}h) = R \quad (1)$$

$$\frac{d\mathbf{u}}{dt} + (\mathbf{u}\nabla)\mathbf{u} + \frac{\nu_t}{h}(h\nabla\mathbf{u}) + g\nabla(h+z) = g\mathbf{S}_f \quad (2)$$

80

81 h is the water depth, $\mathbf{u} = [u_x \quad u_y]^T$ is the depth-averaged flow velocity vector, g is the
 82 acceleration due to gravity, z is the bed elevation, ν_t is the turbulent eddy viscosity, R is the
 83 source/sink term (e.g. rainfall or inflow) and $\mathbf{S}_f = [S_{fx} \quad S_{fy}]^T$ is the bed friction vector.

84 Diffusive wave model neglects all the forces in the momentum equations except for the gravity term
 85 $g\nabla(h+z)$ and bed friction \mathbf{S}_f . The momentum equation Eq. (2) simplifies to:

$$g\nabla(h+z) = g\mathbf{S}_f \quad (3)$$

86 The bed friction can be approximated using Manning's formula:

$$\begin{bmatrix} S_{fx} \\ S_{fy} \end{bmatrix} = \begin{bmatrix} \frac{n^2 |\mathbf{u}| u_x}{h^{4/3}} \\ \frac{n^2 |\mathbf{u}| u_y}{h^{4/3}} \end{bmatrix} \quad (4)$$

87 $\nabla(h+z) = [S_{wx} \quad S_{wy}]^T$ is the water-level surface-gradient vector, where $S_{wx} = d(h+z)/dx$. The

88 modulus of the depth-averaged flow velocity vector is given by:

$$|\mathbf{u}| = \frac{h^{2/3}\sqrt{I_m}}{n} \quad (5)$$

$$I_m^2 = S_{wx}^2 + S_{wy}^2 \quad (6)$$

89

90 2.2. Discretisation of the P-DWave and variable time step

91 The continuity equation Eq. (1) is solved using an explicit first order finite volume discretization on a
92 regular grid. The spatial domain of P-DWave is discretised in cell-centered control volumes:

$$\frac{h_i^{t+1} - h_i^t}{\Delta t} + \frac{1}{A_i} \sum_{j=1}^4 h_{ij} u_{ij} L_{ij} = R \quad (7)$$

93

94 For the sake of simplicity all variables without the time index are evaluated at the current time (t). A_i
95 is the cell-area, L_{ij} is the contact face between cells, u_{ij} and h_{ij} are the water velocity and water-
96 depth at each of the four cell faces evaluated as following:

$$h_{ij} = \frac{h_i + h_j}{2} \quad (8)$$

$$u_{ij} = \frac{h_{ij}^{4/3}}{n_{ij}^2 |\mathbf{u}_{ij}|} I_{n,ij} \quad (9)$$

97

98 u_{ij} is the velocity in the direction perpendicular to each cell face. $I_{n,ij} = (S_{wx}\tilde{n}_x + S_{wy}\tilde{n}_y)_{ij}$ is the
99 water-level surface-gradient vector multiplied with the face unit normal vector $\tilde{\mathbf{n}} = [\tilde{n}_x \quad \tilde{n}_y]^T$.

100 Central schemes are based on local fluxes estimations. The fluxes estimation shown in Eq. (7)

101 requires a lower number of flux evaluations compared with other schemes because the fluxes are

102 averaged at the faces according to Eq. (8) and (9).

103 Explicit schemes must have the time step limited in order to ensure stability. In order to study the
 104 stability of the proposed numerical scheme Eq. (7) is re-written as (for the sake of simplicity R will be
 105 set to zero):

$$h_i^{t+1} = h_i^t \left(1 - \frac{\Delta t}{2A_i} \sum_{j=1}^4 a_{ij} \right) + \frac{\Delta t}{2A_i} \sum_{j=1}^4 a_{ij} h_j^t \quad (10)$$

106

107 Whereby $a_{ij} = u_{ij} L_{ij}$, and after u_{ij} replacement:

$$a_{ij} = \frac{h_{ij}^{2/3} I_{n,ij}}{n_{ij} \sqrt{I_{m,ij}}} L_{ij} \quad (11)$$

108

109 All coefficients in Eq. (10) must be positive in order to ensure that the scheme remains stable and
 110 monotonic:

$$1 - \frac{\Delta t}{2A_i} \sum_{i=1}^4 a_{ij} > 0 \quad (12)$$

111

112 For a regular grid $A_i = \Delta x^2$ the final expression for the variable time step for the x direction can be
 113 obtained by replacing the water-level surface gradient vector in Eq. (11):

$$\Delta t < \text{ArgMax} \left(\text{ArgMin} \left(2\Delta x^2 n_{ij} \frac{\sqrt{S_{wx,ij}}}{h_{ij}^{5/3}} \right), \Delta t_{min} \right) \text{ for all } i, j \quad (13)$$

114

115 A similar expression exists for the y direction. The minimum of both is taken as the final Δt . Eq. (13)
116 is similar to the expressions found in other diffusive models (Hunter *et al.*, 2005; and Cea *et al.*,
117 2010), however herein the smallest allowable time step is twice of those models; the gain comes
118 from the fluxes discretization at the faces (Eq. (8)). Comparing with dynamic models (SWE), the P-
119 DWave time step is proportional to Δx^2 instead of Δx , that means that as long as Δx remains larger
120 than 1 m the P-DWave should be more efficient than the SWE (i.e. having less computational time
121 and increasing quadratically with the cell size). Δt_{min} is justified in order to avoid a too lengthily
122 computational time when $\lim_{S_w \rightarrow 0} \left(2\Delta x^2 n \frac{\sqrt{S_w}}{h^{5/3}} \right) = 0$ and still avoid instabilities when the water is at
123 near rest ($S_w \approx 0$). This solution is similar to the use of tolerance parameters as discussed by Hunter
124 *et al.*(2005); and Cea *et al.* (2010); as such this value should also be decided based on the case study
125 in order not to compromise accuracy. Despite the setting of a Δt_{min} the presented scheme is fully
126 conservative up to machine precision as further discussed in the next sub-section

127

128 **2.3. Process representation of Wet-Dry fronts**

129 During a flooding event there will be inevitably initially dry cells that will switch to a wet state,
130 whereas others will switch from wet to dry as the flood passes. This means that in many situations
131 one must deal with a moving boundary condition. An often found solution when dealing with fixed
132 computational meshes is the use of a depth-threshold or also called wet/dry parameter (Hubbard
133 and Dodd, 2002). This procedure unfortunately adds/removes water to the global system that can
134 either be redistributed to the surrounding cells (Nikolos and Delis, 2009) or negative mass-balance
135 checks need to be incorporate to ensure mass conservation (Liang and Borthwick, 2009).

136 Herein a different approach is presented whereby a ϕ parameter is introduced into the P-DWave
137 continuity equation Eq. (7):

$$\frac{h_i^{t+1} - h_i^t}{\Delta t} + \frac{1}{A_i} \sum_{j=1}^4 \varphi_j h_{ij} u_{ij} L_{ij} = R \quad (14)$$

138

139 In Eq. (14) φ is always set to 1 unless the water depth in the next time step falls below zero140 ($h_i^{t+1} < 0$), in that case φ will take values between $0 < \varphi < 1$ in order to prevent the water-depths

141 from becoming negative. The following condition is applied:

$$\varphi = \varphi_{1...4} = \begin{cases} 1 & \text{for } h_i^{t+1} > 0 \\ \frac{\Delta x^2}{\Delta t} \frac{h_i^t + R\Delta t}{\sum_{j=1}^4 h_{ij} u_{ij} L_{ij}} & \text{for } h_i^{t+1} < 0 \end{cases} \quad (15)$$

142

143 Eq. (15) allows the model to remain fully conservative up to machine precision. This is clear since φ 144 parameter is updated for all 4 faces belonging to the cell ($\varphi_{1...4}$) enabling neighbouring cells to use145 the corrected φ , avoiding negative water-depths and water gains or losses. Bradbrook et al. (2013)

146 presented a similar approach but the scaling of the fluxes was still dependent on a minimum depth

147 greater than 0 and absolute mass conservation was not attained.

148

149 **2.4. Parallel implementation of the code**

150 The code is implemented in both Matlab and Fortran environment. Fortran parallelization is achieved

151 by implementing OpenMP Application Programming Interface (API) directives. OpenMP API is

152 preferred to an MPI approach due to its ease of implementation with minimal changes to the non-

153 parallel version. Regarding Matlab, vectorised operations are used whenever possible to improve

154 modelling efficiency. Vectorised code is more efficient than the traditional do-loop iterations;

155 however not all computing steps are able to be vectorised. In the latter case, we take advantage of

156 modern multi-CPUs and multicores and adopted the built-in parallel computing toolbox in the
157 Matlab to accelerate the computation.

158 The Matlab parallel computing toolbox provides several functions to use multicore processors,
159 including parfor loop, GPU computing, spmd (single program multiple data), etc. When applying
160 parfor loops, 2D arrays need to be sliced into multiple arrays such that each WORKER¹ can update
161 the variable to the sliced array without causing problems in the shared memory. After each iteration
162 the sliced arrays are gathered back into the original 2D array such that all WORKERS can compute
163 with the correct updated array in the next iteration.

164 It should be noted that we also tested spmd approach (Matlab) on a multicore desktop but found
165 the benefit to be limited on the shared memory computer. The application of spmd performs better
166 on a distributed memory framework, which requires more attention on domain decomposition to
167 ensure the optimum balance of load among computing nodes, and the minimum data to be
168 synchronised. In the algorithm, the calculation of a cell requires information from its neighbour cells
169 such that addition information of cells surrounding the decomposed domain is needed, which makes
170 the domain decomposition a more complex task. Therefore, we leave the spmd implementation for
171 a future stage when simulations with large scale data on distributed machines are required.

172

173 **3. Model Testing: results and discussion**

174 To assess the model performance seven tests are selected which enable studying specific flooding
175 aspects and verify the model accuracy. The first and second tests were first presented in Hunter et
176 al. (2005) and allow testing the model accuracy in propagating an inundation front. Third, fourth and
177 fifth tests are taken from the Benchmark tests carried out by the UK Environmental Agency (EA) and
178 allow a direct comparison with existing diffusive and dynamic models (Pender and Néelz, 2010).

¹ WORKER is the terminology used in Matlab to refer to a thread, i.e. the maximum number of processes that can be run simultaneously during a parallel session.

179 Computational times are additionally given to allow the reader to compare them with the various
 180 models ran in the EA. The sixth test was first presented by Wasantha Lal (1998). This test aims to
 181 quantitatively assess the model's accuracy in propagating an inundation front in a 2D space. In the
 182 original paper the Authors offered a way to obtain a solution against which numerical models can be
 183 compared to. In the seventh and last test we recover the Wasantha Lal (1998) test to verify the
 184 efficiency of the Parallel coding. Herein computational times are also disclosed.

185

186 **3.1. Horizontal plane wetting**

187 The horizontal plane wetting test performed in a horizontal 5km long rectangular channel (slope=0)
 188 aims to test the model accuracy in propagating an inundation front. Hunter et al. (2005) showed that
 189 by considering a constant inflow at the left boundary it is possible to simplify the SWE and obtain an
 190 analytical solution. All boundary conditions are defined as closed except for the left boundary. The
 191 left boundary condition is obtained by setting the horizontal coordinate x equal to 0 in the analytical
 192 solution. The final expression for the boundary condition is presented in Eq. (16) :

$$\begin{aligned}
 h_1^t &= \left[\frac{7}{3} (0.07 + n^2 u_1^3 t) \right]^{3/7} \quad (m) \\
 u_1^t &= 1 \quad (m/s)
 \end{aligned}
 \tag{16}$$

193

194 Five different domains are defined in order to analyse the sensitivity of the model to the number of
 195 cells, CellNo={200, 100, 50, 25} (grid resolution of Δx ={25, 50, 100, 200} m). Five corresponding
 196 smallest allowable time steps are defined to each domain Δt_{min} ={0.001, 0.05, 0.5, 1.0} s such that
 197 the variable time step remains smooth and the solution free of instabilities. The Manning's
 198 coefficient=0.01 $m^{-1/3}/s$.

199 **Figure 1** compares the evolution of the Water-surface level for eight time steps predicted by the
 200 Model and the analytical solution. The P-DWave solution produces a water level profile consistent
 201 with the analytical solution across all number of cells discretized CellNo={200, 100, 50, 25} (grid
 202 resolution of $\Delta x = \{25, 50, 100, 200\}$ m). Naturally as the number of cells decreases the ability to
 203 represent the curved stepped front is slightly impaired. Nonetheless the front location does not
 204 show signs of overshooting or delay. As discussed in **section 2.2** depending on the case study it may
 205 be required testing different Δt_{min} in order to find a solution with the wished level of accuracy.
 206 **Figure 2** shows a smooth evolution of the time step with the iteration number (it). For the finer cell
 207 resolutions CellNo={200, 100} ($\Delta x = \{25, 50\}$) Eq. (13) controls the maximum allowable time step. For
 208 CellNo={50, 25} ($\Delta x = \{100, 200\}$) a maximum time step of 1 sec is imposed to provide a detailed
 209 output of the solution. The latter has no effect on the accuracy of the model since 1 sec is smaller
 210 than the maximum allowable time step. Quantitatively, **Table 1** presents the Root Mean Square
 211 Error (RMSE) errors statistics of the Model solution compared with the analytical solution. The errors
 212 remain small across all solutions; the error exhibits similar behaviour and magnitudes to those
 213 obtained by Hunter et al. (2005).

214

215 **3.2. Inundation “wetting and drying” of a planar beach $S \neq 0$**

216 The inundation “wetting and drying” test of a planar beach with $S \neq 0$ allows testing the model ability
 217 to simulate advancing and receding of an inundation front. The test consists of a 5 km long channel
 218 with a slope of 0.001, whereby the left boundary condition is defined by a sinusoidal wave of
 219 amplitude 4m and 3000 sec period, as seen in Eq. (17).

$$h_1^t = 4 \sin\left(t \frac{\pi}{3000}\right) (m) \quad (17)$$

$$u_1 = 1 (m/s)$$

220

221 In order to analyse the sensitivity of the Model to Manning's coefficient, four different values are
222 simulated $n=\{0.01,0.02,0.04,0.08\} m^{-1/3}s$. The domain is discretised with 100 cells with $\Delta x=50$ m,
223 and the smallest allowable time step Δt_{min} is equal to 0.001 s. **Figure 3** shows the evolution of the
224 Water-surface level for eight time steps predicted by the Model for the four tested Manning values.
225 Although there is no analytical solution, the shape and front propagation is intuitively correct as it
226 shows a marked step front which is delayed with the increase of the Manning's coefficient and its
227 behaviour is similar to the solution found in Hunter et al. (2005). This test case is nonetheless more
228 demanding than the previous one because a nearly flat surface appears at $x=0$ m and becomes more
229 pronounced before and after the receding phase (i.e. between $t=1100$ s and $t=1900$ s). The variable
230 time step in **Figure 4** shows a controlled jerky oscillation indicating that the time step has reached
231 the smallest allowable time step. As the Manning's coefficient is increased the required time step
232 becomes larger than Δt_{min} (as defined in Eq. (13)) and the oscillatory behaviour disappears.

233 In the absence of an analytical solution, and in order to decide an acceptable value for the smallest
234 allowable time step, a sensitivity analysis of the Model to Δt_{min} is sought. Here four different
235 $\Delta t_{min}=\{0.001, 0.01, 0.1, 1\}$ s are compared with $\Delta t_{min}=0.0005$ s. **Table 2** shows the corresponding
236 RMSE (m) error statistics for four instants in time. In this case the error is calculated assuming that
237 the solution with $\Delta t_{min}=0.0005$ s is our true solution. It is clear that as Manning's coefficient reduces
238 the Δt_{min} required becomes smaller; this is in line with Eq. (13). It is also noteworthy that the higher
239 errors are found between $t=1100$ s and $t=1900$ s during the rising limb of the inundation front,
240 clearly signalling that the smallest allowable time step has been reached and it should be decreased.

241 For Δt_{min} smaller than 0.01 s the RMSE become negligible. Finally after the receding phase (or
242 falling limb), the model recovers and reduces its RMSE. This rather surprising result can be partially
243 explained by the wetting and dry treatment used herein; using Eq. (15) mass conservation is always
244 ensured such that the actual volume of water within the model remains always correct. Depending

245 on a favourable variation of the boundary conditions (such as in this test) it is possible that the
 246 model recovers to a state closer to the correct solution.

247

248 3.3. Flooding a disconnected water body test

249 This test is retrieved from the EA benchmarking test. It allows assessing the accuracy of the model to
 250 handle disconnected water bodies, and the wetting and drying of floodplains. The domain is defined
 251 by a rectangular channel of $100 \times 700 \text{ m}^2$ with a Manning's coefficient $= 0.03 \text{ m}^{-1/3} \text{ s}$ and discretised
 252 into $\text{CellNo} = 10 \times 70$ cells ($\Delta x = 10 \text{ m}$). Δt_{\min} is set to 0.05 s and the maximum time step is set to 10 s.
 253 The left boundary condition is an inflow hydrograph specified by water levels in Eq.(18):

$$h_{ij}^t + z_{ij}^t = \begin{cases} 9.7 & \text{for } t = 0 \\ 9.7 + \frac{0.65}{3600}t & \text{for } t < 3600 \\ 10.35 & \text{for } t = [3600, 36960] \\ 10.35 - \frac{0.65}{6240}(t - 36960) & \text{for } t = [36960, 43200] \\ 9.7 & \text{for } t > 43200 \end{cases} \quad (18)$$

254 The profile of the digital elevation model and the water-surface levels predicted by P-DWave at two
 255 specific points along the channel are presented in **Figure 5**. In addition the results from the various
 256 models in the EA are superimposed in order to enable easy accuracy comparison.

257 In terms of accuracy, P-DWave predicted the beginning of the flow in Point 1 starting at
 258 approximately one hour and reaching the maximum water level after approximately four hours. The
 259 water level rise and receding (starting at hour 12) are also predicted in good agreement with all
 260 other models (see e.g. ISIS 2D dynamic model ("Wallingford Software Ltd," 2006) or the UIM
 261 diffusive wave model (Chen *et al.*, 2005)). It is reasonable to conclude that the inertial terms could
 262 indeed be neglected as no obvious improvement in the results is seen by the dynamic models. In
 263 terms of computing time, P-DWave run is completed after 173 s (models' times in the EA report
 264 vary between 1 s and 349 s), with a total number of 1410303 computational time steps, the

265 observed average time step is 0.051 s which indicated that the model is for the most of the
 266 computational time steps equal to $\Delta t_{min} = 0.05$ s.

267

268

269 3.4. Filling of floodplain depressions

270 This test aims to assess the model's ability to predict the inundation extent on a complex topography
 271 and to handle disconnected water bodies. The domain is defined by a squared area of 2000x2000 m²
 272 with a Manning's coefficient=0.03 m^{-1/3}/s and discretised into CellNo=100x100 cells ($\Delta x=20$ m).
 273 The maximum time step is set to 10 s and Δt_{min} is set to 1.0 s The boundary condition is an inflow
 274 hydrograph (Q_{ij}^t) at the top left corner defined by Eq. (19):

$$Q_{ij}^t = \begin{cases} 0 & \text{for } t = [0, 300] \\ 0 + \frac{20}{300}(t - 300) & \text{for } t < 600 \\ 20 & \text{for } t = [600, 5160] \\ 20 - \frac{20}{30}(t - 5160) & \text{for } t = [5160, 5460] \\ 0 & \text{for } t > 5460 \end{cases} \quad (19)$$

275

276 The final distribution of the flood inundation extent is consistent with that predicted by the full
 277 dynamic models used in the B-EA (**Figure 6**), as well as the filling up sequence and time as can be
 278 seen in the final water level points presented in **Figure 7**. The travels times in Points 4 and 2 are
 279 again consistent with all models, however some delay on the flood front can be observed in the
 280 points located further away from the inflow point (e.g. Point 10) as well as a slight overshoot of the
 281 flood peak in Point 4. It should be noted that while the overshoot is more noticeable in diffusive
 282 models's results (e.g. UIM; Chen *et al.*, 2005) similar delays can also been seen in the dynamic
 283 models' results (e.g. JFLOW+; Bradbrook, 2006). Point 9 is never inundated as expected. Overall, the
 284 results support that the diffusive equations are indeed sufficient to simulate this test case. P-DWave

285 run takes 110 s to complete (EA models' times vary between 1 s and 1130 s), with 172224
286 computational time steps and an average time step of 1.001 s.

287

288 **3.5. Rainfall and point source surface flow in urban areas**

289 This test aims to assess the model's ability to simulate shallow inundation from a point source and
290 from rainfall. The domain is defined by an area of $0.4 \times 0.96 \text{ m}^2$ with a Manning's coefficient = 0.03
291 $\text{m}^{-1/3}/\text{s}$ for roads and pavements, and $0.05 \text{ m}^{-1/3}/\text{s}$ elsewhere. The domain is discretised into
292 $\text{CellNo} = 483 \times 201$ cells ($\Delta x = 2 \text{ m}$) (**Figure 8**). The maximum time step is set to 10 s and Δt_{\min} is set to
293 0.03 s. The point source boundary condition is an inflow hydrograph (please refer to Pender and
294 Néelz (2010)) and a uniform rainfall of 400 mm/h with 4 min duration and starting at minute 1. Total
295 simulation time is 5 h.

296 In terms of the final flood inundation extent the results are consistent with that predicted by the full
297 dynamic models (**Figure 8**), although there are some differences in the maximum water levels
298 reached which remain nonetheless within 0.1 m (**Figure 9**). The differences are more obvious during
299 the second flood peak caused by the inflow hydrograph in Points 1 and 2. As in the previous example
300 similar behaviour is found in other diffusive models (e.g. UIM; Chen *et al.*, (2005) and RFSM;
301 Jamieson *et al.*, (2012)). Overall, the flood peak times and water levels are within the limits predicted
302 by the models in EA. P-DWave run takes 10378 s to complete (EA models' times vary between 1 s
303 and 18470 s), with 596795 computational time steps and an average time step of 0.0301 s.

304

305 **3.6. Axisymmetric test**

306 The Axisymmetric test allows testing the accuracy of the model to propagate an inundation front in a
307 two-dimensional space (2D). The domain is defined by a squared area of $160.93 \times 160.93 \text{ km}^2$ with a

308 Manning's coefficient= $1.0 \text{ m}^{-1/3}/\text{s}$ and discretised in CellNo=50x50 cells ($\Delta x = 3218.7 \text{ m}$). The initial
 309 condition is a smooth cosine function as defined by Eq. (20):

310

$$h_{ij}^1 = \left[0.4575 + 0.1525 \cos\left(\frac{\pi r_{ij}}{r_{max}}\right) \right] (m) \quad \text{for } r_{ij} \leq r_{max} \quad (20)$$

$$h_{ij}^1 = 0.305 (m) \quad \text{otherwise}$$

311

312 In Eq. (20) r_{ij} is the distance of each grid point from the domain centre with a $r_{max} = 32.188 \text{ m}$.
 313 Due to its symmetry around the axis it is possible to derive an axisymmetric continuity equation for
 314 shallow water flows. The modified 1D diffusion equation can then be solved using a very fine grid
 315 with fix $\Delta t = 26\text{s}$ and compared with the 2D model as in Wasantha Lal (1998). The solution from this
 316 fine model is termed herein the Axisymmetric solution.

317 The water-surface level and velocity fields are shown in **Figure 10** for four time steps $t=\{2, 3, 9, 12\}$
 318 (t is here represented in days (d)) predicted by the model for four different smallest allowable time
 319 steps $\Delta t_{min}=\{100, 500, 2000, 8000\}$ s and compared with the Axisymmetric solution. The model
 320 solution is in good agreement with the Axisymmetric solution with a slight smoothing of the solution
 321 for higher Δt_{min} ; this can also be inferred by the RMSE error statistics in **Table 3** which exhibit
 322 smaller errors than the numerical solutions obtained by Wasantha Lal (1998). The velocity fields
 323 show that the solution remains symmetric in respect to both axis with time. Also noteworthy are the
 324 velocity low values of this particular test due to the high Manning's coefficient used².

325 It is clear that Δt_{min} is the dominant restriction in Eq. (13). **Figure 11** shows that as Δt_{min} reduces,
 326 the variable time step is subsequently reduced. Despite the fact that the variable time step is often

² In the Author's opinion, the Manning's value is unrealistically high and can only be justified by the large $\Delta x = 3218.7 \text{ m}$ which would then encompass the added roughness by houses, roads and other overland flow obstructions.

327 equal to Δt_{min} and not the one obtained through the stability analysis in Eq. (12), **Figures 10 and 11**
 328 show that it is possible that the model simulation still converges to the correct solution. There are
 329 nonetheless, some visible oscillations in the water level for the larger $\Delta t_{min}=8000$ s. This test will
 330 also be used in **Section 3.7** for testing the efficiency of the parallelization coding of the model.

331

332 **3.7. Parallel performance test: Speed-up and efficiency**

333 The final test has the objective of verifying the parallel performance. The test in **section 3.6** is here
 334 recovered because it uses a 2D mesh and it is easily scalable. In **section 3.6** a mesh with
 335 CellNo=50x50 cells was used, herein we will test four different CellNo={300x300, 500x500, 700x700,
 336 900x900} ($\Delta x = \{536.4, 321.9, 229.9, 178.8\}$ m) with $\Delta t_{min}=500$ s. In order to compare and verify the
 337 parallel performance we raise the number of cells and therefore increase the computational effort
 338 by a quadratic exponent (see Eq. (14)). The two common metrics used in this paper are speed-up
 339 and efficiency (**Table 4**) and follow the notation by Yu (2010). Speed up is defined as the ratio
 340 between the single processor execution time and that of the multi-processor:

$$Sp(nc, P) = \frac{T_{Single}(nc)}{T_{multiple}(nc, P)} \quad (21)$$

341

342 In Eq. (21) $T_{Single}(nc)$ is the run time of the sequential algorithm, and $T_{multiple}(nc, P)$ is the run
 343 time of the parallel algorithm using P core-processors. Efficiency is defined by Eq. (22):

$$E(nc, P) = \frac{Sp(nc, P)}{P} \quad (22)$$

344

345 The total run time is set to 1 hour since we are only focusing on the computational efficiency of the
346 model. The tests were conducted on a workstation with AMD Opteron™ Processor 6276 with 12
347 cores 2.3GHz CPU and 192GB of RAM at RUHR University of Bochum.

348 It is interesting to notice that although Matlab computational times are larger than Fortran, Matlab
349 speed-up performs better than Fortran. Two possible explanations could be the highly efficient
350 Fortran code which sees smaller gains through parallelizing than Matlab or that a more complex
351 Fortran MPI approach is required to increase the gains in speed-up closer to Matlab performance. In
352 any case it is clear that the model developed is indeed scalable. It is also noteworthy that depending
353 on the CellNo and the measure adopted to describe efficiency, the optimal use of number of
354 processors might be different. Purely looking at the computational time it seems obvious that the
355 maximal possible number of processers should always be selected; however once one focus on the
356 speed-up, it becomes obvious that there is an improvement limit, simply because the
357 communication costs between processors becomes too high (Yu, 2010). In that case Efficiency can
358 be a simple way to decide on the number of processors to use. For example, if one selects a
359 minimum efficiency of 0.75 and the Matlab code two processors would be the optimal choice for
360 CellNo=300x300, four processors would only be worth it from CellNo=700x700 and for 12 processors
361 a much larger CellNo would be necessary.

362 Lastly, it is worth mentioning that the speedup and efficiency obtained herein with the Matlab code
363 exhibit a behaviour similar (and magnitudes) to the ones obtained by Yu (2010) and Neal, Fewtrell, &
364 Trigg (2009). Future work will see the implementation of the MPI approach using Fortran.

365

366 **4. Conclusion**

367 In this paper we presented a parallelized two-dimensional diffusive wave model (P-DWave) with
368 adaptive time step. The parallelization was achieved in the Matlab environment with the use of the
369 parfor loop, and using computational vectorization whenever possible, while in Fortran it was

370 achieved using OpenMP API. The model was validated in seven tests against known analytical
371 solutions, and diffusive and dynamic models results from an EA benchmark report. The model
372 converged regardless of the spatial resolution as long as the selected minimum step was not too
373 limiting (this limit is found to be case study dependent), and showed sensitivity to the changes of
374 Manning's roughness in a sloped planar beach. Symmetry was kept in the test case of a horizontal
375 plane, and the model was proven robust even in the presence of strong irregular geometries. The
376 process devised to represent Wet-Dry fronts was effective in keeping a sharp front, while the
377 variable time step kept the solution stable and oscillations-free in all tests

378 The parallelization strategy was indeed effective, by improving the speed-up times from 1.7 to 5.1
379 and from 1.2 to 1.7 respectively for Matlab and Fortran, depending on the domain size and the
380 number of processors used. The speed-up increases as the domain size becomes larger or the
381 number of processors progressively increases. Efficiency follows a similar trend in relation to the
382 domain size increase, but it can half its value as the number of processors change from 2 to 12
383 processors. Similarly to other Authors' results this is attributed to the communication costs between
384 processors. Future work may see the parallelization of this same code in a different programming
385 language or using another parallelization strategy to analyse the potential benefits, and inclusion of
386 the dynamic terms in the code developed for a thorough discussion on the differences in
387 computational run times.

388

389 **5. Acknowledgments**

390 The Authors would like to acknowledge the support of the DFG - Deutsche Forschungsgemeinschaft -
391 through Project GZ: LE 3220/1-1. Three anonymous reviewers are also acknowledged for their
392 valuable comments and suggestions on an early version of this paper. The authors would also like to
393 thank the UK Environment Agency for the EA benchmarks datasets.

394

395 **6. References**

- 396 Bates, P.D., Horritt, M.S., Fewtrell, T.J., 2010. A simple inertial formulation of the shallow water
397 equations for efficient two-dimensional flood inundation modelling. *J. Hydrol.* 387, 33–45.
- 398 Bates, P.D., Roo, A.P.J. De, 2000. A simple raster-based model for flood inundation simulation. *J.*
399 *Hydrol.* 236, 54–77.
- 400 Bradbrook, K., 2006. JFLOW: a multiscale two-dimensional dynamic flood model. *Water Environ. J.*
401 20, 79–86.
- 402 Bradbrook, K.F., Lane, S.N., Waller, S.G., Bates, P.D., Consulting, J.B.A., Barn, S., Hall, B., Yorkshire, N.,
403 2013. Two dimensional diffusion wave modelling of flood inundation using a simplified channel
404 representation. *Int. J. River Basin Manag. Taylor* 2 (3), 37–41.
- 405 Burger, G., Rauch, W., 2012. Parallel Computing in Urban Drainage Modeling : A Parallel Version of
406 EPA SWMM. UDM 2012, Belgrade, Serbia 1–9.
- 407 Cea, L., Garrido, M., Puertas, J., 2010. Experimental validation of two-dimensional depth-averaged
408 models for forecasting rainfall–runoff from precipitation data in urban areas. *J. Hydrol.* 382,
409 88–102.
- 410 Ceyhan, E., Ou, S., Estrade, B., Kosar, T., 2007. Towards a faster and improved ADCIRC (ADvanced
411 Multi-Dimensional CIRCulation) model. *J. Coast. Res. Special Is.*
- 412 Chen, A.S., Evans, B., Djordjević, S., Savić, D.A., 2012. Multi-layered coarse grid modelling in 2D
413 urban flood simulations. *J. Hydrol.* 470–471, 1–11.
- 414 Chen, A.S., Hsu, M.H., Chen, T.S., Chang, T.J., 2005. An integrated inundation model for highly
415 developed urban areas. *Water Sci. Technol.* 51, 221–9.
- 416 Da Paz, A.R., Collischonn, W., Bravo, J.M., Bates, P.D., Baugh, C., 2013. The influence of vertical water
417 balance on modelling Pantanal (Brazil) spatio-temporal inundation dynamics. *Hydrol. Process.*
- 418 Di Baldassarre, G., Schumann, G., Bates, P.D., 2009. A technique for the calibration of hydraulic
419 models using uncertain satellite observations of flood extent. *J. Hydrol.* 367, 276–282.
- 420 Dottori, F., Baldassarre, D., Todini, E., 2013. Detailed data is welcome, but with a pinch of salt:
421 accuracy, precision, and uncertainty in flood inundation modeling. *Water Resour. Res.* 49,
422 6079–6085.
- 423 Dottori, F., Todini, E., 2011. Developments of a flood inundation model based on the cellular
424 automata approach: Testing different methods to improve model performance. *Phys. Chem.*
425 *Earth, Parts A/B/C* 36, 266–280.
- 426 Hirsch, C., 2007. Numerical computation of internal and external flows. The fundamentals of
427 computational fluid dynamics, second. ed. Elsevier, Butterworth-Heinemann.

- 428 Horritt, M.S., 2006. A methodology for the validation of uncertain flood inundation models. J.
429 Hydrol. 326, 153–165.
- 430 Hubbard, M.E., Dodd, N., 2002. A 2D numerical model of wave run-up and overtopping. Coast. Eng.
431 47, 1–26.
- 432 Hunter, N.M., Horritt, M.S., Bates, P.D., Wilson, M.D., Werner, M.G.F., 2005. An adaptive time step
433 solution for raster-based storage cell modelling of floodplain inundation. Adv. Water Resour.
434 28, 975–991.
- 435 Hunter, N.M., Villanueva, I., Pender, G., Lin, B., Mason, D.C., Falconer, R. a., Neelz, S., Crossley, a. J.,
436 Bates, P.D., Liang, D., Wright, N.G., Waller, S., 2008. Benchmarking 2D hydraulic models for
437 urban flooding. Proc. ICE - Water Manag. 161, 13–30.
- 438 Jamieson, S.R., Wright, G., Lhomme, J., Gouldby, B.P., 2012. Validation of a computationally efficient
439 2D inundation model on multiple scales. FloodRisk 2012, Novemb. 2012, Rotterdam. 20–22.
- 440 Judi, D., Burian, S., McPherson, T., 2011. Two-dimensional fast-response flood modeling: desktop
441 parallel computing and domain tracking. J. Comput. Civ. Eng. 25, 184–191.
- 442 Liang, Q., Borthwick, A.G.L., 2009. Adaptive quadtree simulation of shallow flows with wet–dry
443 fronts over complex topography. Comput. Fluids 38, 221–234.
- 444 Maksimovic, C., Prodanović, D., 2001. Modelling of urban flooding—breakthrough or recycling of
445 outdated concepts. Urban Drain. Model. 1–9.
- 446 Mark, O., Weesakul, S., Apirumanekul, C., Aroonnet, S.B., Djordjević, S., 2004. Potential and
447 limitations of 1D modelling of urban flooding. J. Hydrol. 299, 284–299.
- 448 Neal, J., Fewtrell, T., Trigg, M., 2009. Parallelisation of storage cell flood models using OpenMP.
449 Environ. Model. Softw. 24, 872–877.
- 450 Neal, J., Villanueva, I., Wright, N., Willis, T., Fewtrell, T., Bates, P., 2012. How much physical
451 complexity is needed to model flood inundation? Hydrol. Process. 26, 2264–2282.
- 452 Nikolos, I.K., Delis, A.I., 2009. An unstructured node-centered finite volume scheme for shallow
453 water flows with wet/dry fronts over complex topography. Comput. Methods Appl. Mech. Eng.
454 198, 3723–3750.
- 455 Pender, G., Néelz, S., 2010. Benchmarking of 2D hydraulic modelling packages. SC080035/R2
456 Environ. Agency Bristol 169 pp.
- 457 Prestininzi, P., 2008. Suitability of the diffusive model for dam break simulation: Application to a
458 CADAM experiment. J. Hydrol. 361, 172–185.
- 459 Rossman, L.A., 2005. Storm water management model - user's manual Version 5.0. EPA - United
460 States, EPA - United States, Cincinnati
461 <http://www.epa.gov/ednrmrl/models/swmm/epaswmm5-m>.
- 462 Wallingford Software Ltd, 2006. . ISIS Flow / Hydrol.
463 <http://www.wallingfordsoftware.com/products/isis/>.

464 Wasantha Lal, A.M., 1998. Performance comparison of overland flow algorithms. *J. Hydraul. Eng.*
465 124, 342–349.

466 Yu, D., 2010. Parallelization of a two-dimensional flood inundation model based on domain
467 decomposition. *Environ. Model. Softw.* 25, 935–945.

468 Zhang, X.D., Trepanier, J.-Y., Reggio, M., Camarero, R., 1994. Time-accurate local time stepping
469 method based on flux updating. *Fluid Mech. Heat Transf.* 32, 1926–1928.

470

471

472

ACCEPTED MANUSCRIPT

473 **Figures**

474

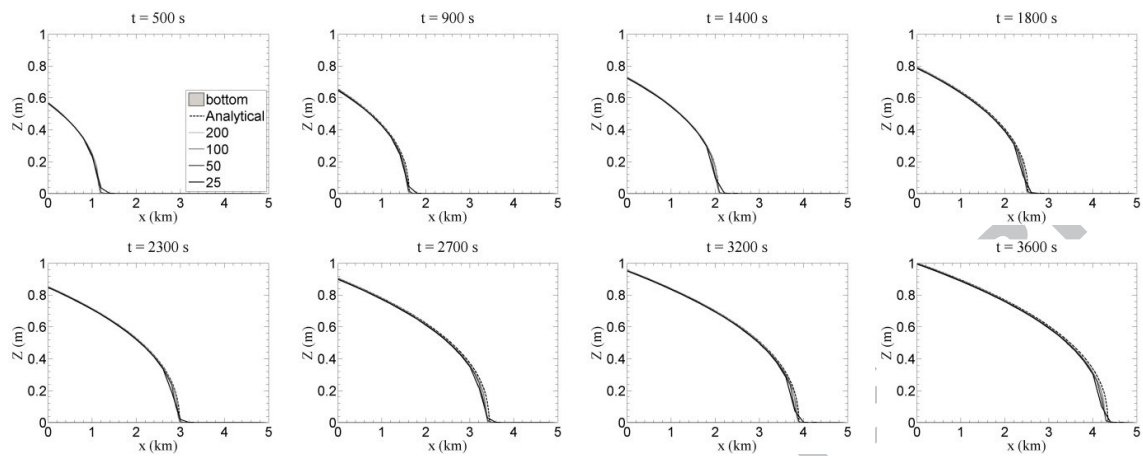


Figure 1. Water-surface level for the “horizontal plane wetting” test predicted by P-DWave and the analytical solution (dashed line). Sensitivity analysis to the number of cells $CellNo=\{200, 100, 50, 25\}$ ($\Delta x=\{25, 50, 100, 200\}$ m) with $\Delta t_{min}=\{0.001, 0.05, 0.5, 1.0\}$ s on the front propagation.

475

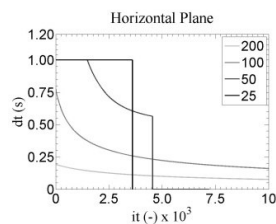


Figure 2. Evolution of the time step solution with the iteration number (it) as a function of the number of cells discretised $CellNo=\{200, 100, 50, 25\}$ ($\Delta x=\{25, 50, 100, 200\}$ m) with $\Delta t_{min}=\{0.001, 0.05, 0.5, 1.0\}$ s during the horizontal plane wetting simulation.

476

477

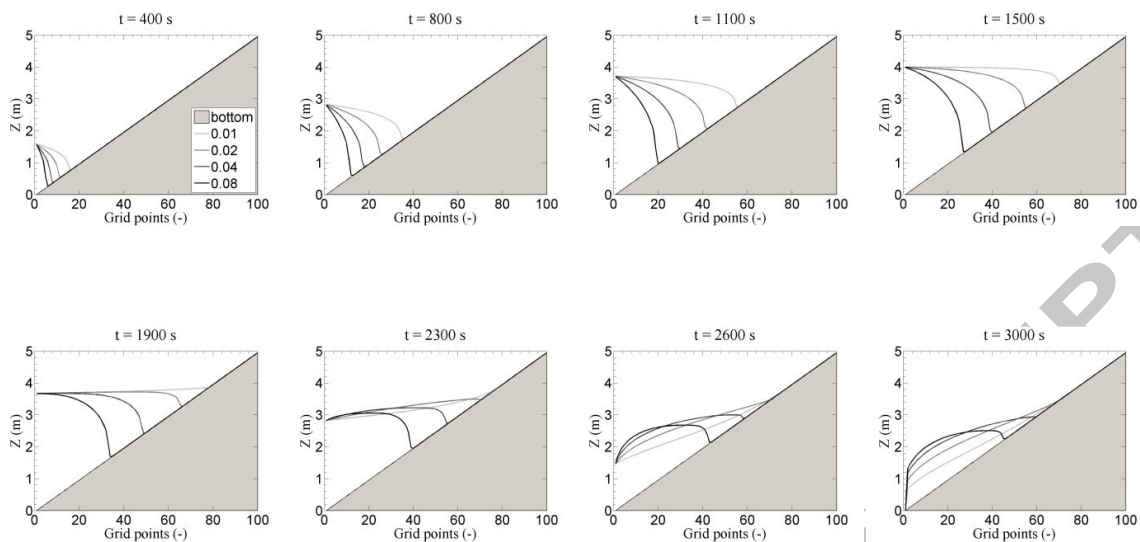


Figure 3. Sensitivity analysis of the predicted water-surface level propagation to Manning's coefficient for the "inundation of a planar beach" $S \neq 0$ test ($\Delta x = 50$ m and $\Delta t_{\min} = 0.001$ s).

478

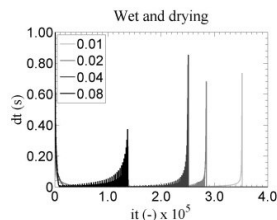


Figure 4. Evolution of the time step solution with the iteration number (it) as a function of Manning's coefficient $n = \{0.01, 0.02, 0.04, 0.08\} m^{-1/3} s$ and $\Delta t_{\min} = 0.001$ s during the Inundation of a planar beach $S \neq 0$ simulation.

479

480

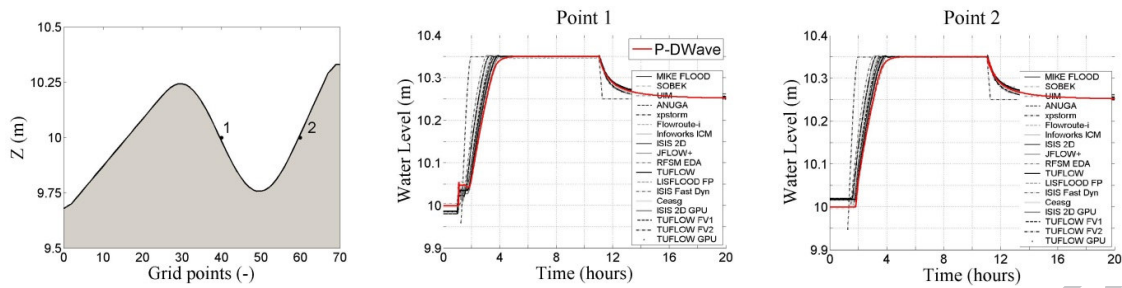


Figure 5. Profile of the digital elevation model (DEM) (left). Water-surface levels at points 1 and 2 for the “flooding a disconnected water body” test predicted by P-DWave and superimposed with the various models’ results published in the EA benchmark (Pender and Néelz, 2010) test for comparison (middle and right).

481

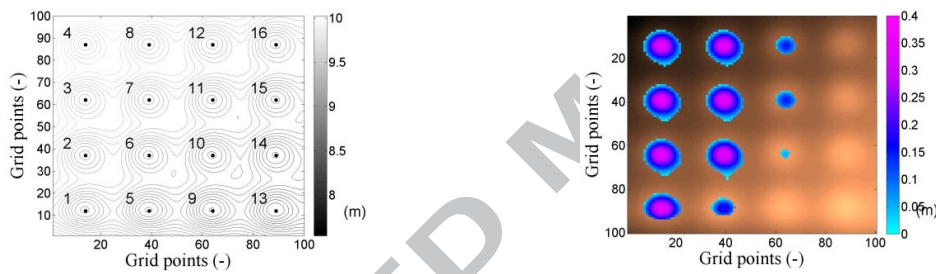


Figure 6. Map of the DEM showing the points locations where water levels are recorded (left). Final inundation predicted by P-DWave (right).

482

483

484

485

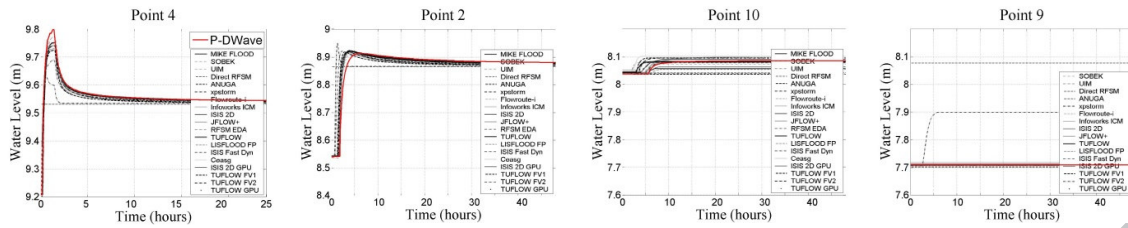


Figure 7. Water-surface level for the “filling of floodplain depressions” test predicted by P-DWave superimposed with the results from the models published in the EA benchmark (Pender and Néelz, 2010) test for comparison.

486

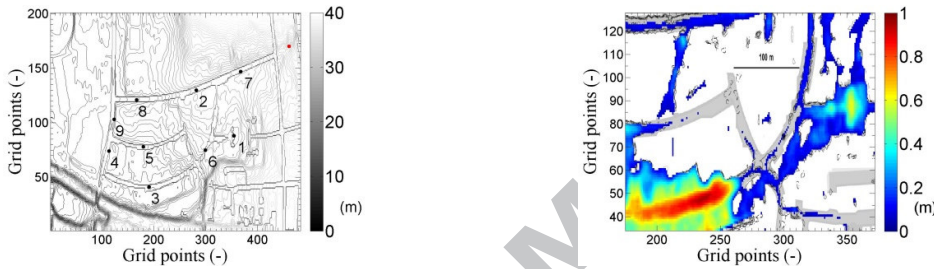


Figure 8. Map of the DEM showing the points locations where water levels are recorded (black dots) and the inflow hydrograph location (red dot) (left). Final Inundation predicted by P-DWave overlapped with the models’s flood extents in the EA report (Pender and Néelz, 2010) (right).

487

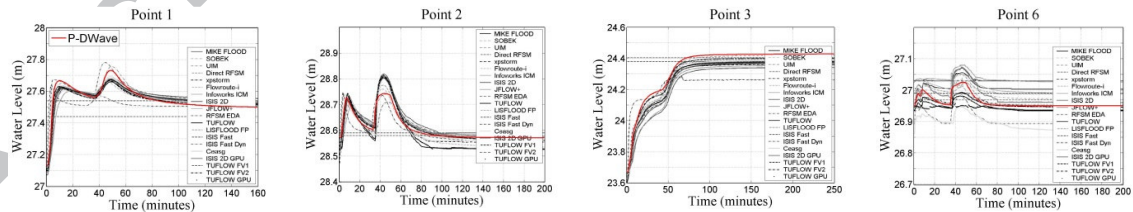


Figure 9. Water-surface level for the “rainfall and point source surface flow in urban areas” test predicted by P-DWave superimposed with the results from the models published in the B-EA test (Pender and Néelz, 2010).

488

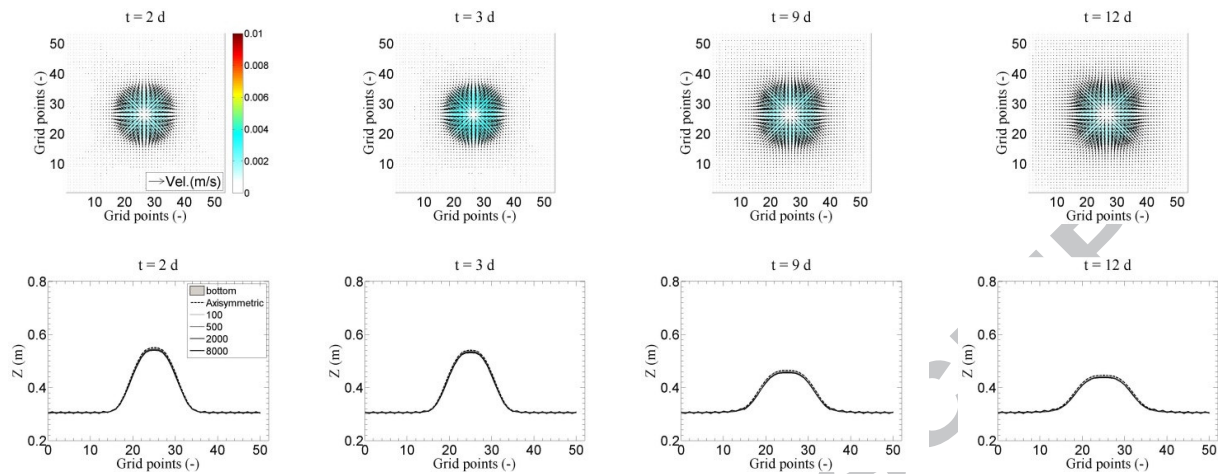


Figure 10. Water-surface level and velocity fields ($\Delta t_{min}=100$ s) for the “Axisymmetric” test predicted by the P-DWave and the Axisymmetric model solution (dashed line) on the front propagation. Sensitivity analysis of the water-surface centre profile for $\Delta t_{min}=\{100, 500, 2000, 8000\}$ s and CellNo=50x50 ($\Delta x = 3218.7$ m).

489

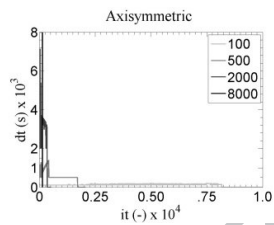


Figure 11. Evolution of the time step solution with the iteration number (it) as a function of the smallest allowable time step $\Delta t_{min}=\{100, 500, 2000, 8000\}$ s with CellNo=50x50 ($\Delta x = 3218.7$ m) during the Axisymmetric test.

490

491

492 **Tables**

493

494 **Table 1.** RMSE (m) statistics for the “horizontal plane wetting” predicted by using CellNo={200, 100,
 495 50, 25} (grid resolution of Δx ={25, 50, 100, 200} m) with Δt_{min} ={0.001, 0.05, 0.5, 1.0} s compared
 496 with the analytical solution for 8 instants in time.

RMSE (m)	t (s)								
	CellNo	500	900	1400	1800	2300	2700	3200	3600
200	0.005	0.007	0.009	0.010	0.012	0.013	0.015	0.016	
100	0.010	0.013	0.016	0.018	0.022	0.025	0.027	0.030	
50	0.019	0.025	0.031	0.034	0.040	0.045	0.050	0.054	
20	0.028	0.038	0.048	0.058	0.065	0.077	0.084	0.093	

497

498

499

500

501

502

503

504

505

506

507 **Table 2.** RMSE (m) statistics for the “inundation of a planar beach” $S \neq 0$ predicted by using
 508 $\Delta t_{min} = \{0.001, 0.01, 0.1, 1\}$ s and $n = \{0.01, 0.02, 0.04, 0.08\} m^{-1/3} s$ compared with $\Delta t_{min} = 0.0005$ s, for
 509 four instants in time.

RMSE (m)	t = 400 s				t = 1100 s			
	Δt_{min} (s)				Δt_{min} (s)			
n ($s/m^{1/3}$)	0.001	0.01	0.1	1	0.001	0.01	0.1	1
0.01	0.000	0.000	0.000	0.245	0.000	0.000	0.515	1.357
0.02	0.000	0.000	0.000	0.016	0.000	0.000	0.004	1.009
0.04	0.000	0.000	0.000	0.002	0.000	0.000	0.000	0.552
0.08	0.000	0.000	0.000	0.000	0.000	0.000	0.000	0.017

510

RMSE (m)	t = 1900 s				t = 3000 s			
	Δt_{min} (s)				Δt_{min} (s)			
n ($s/m^{1/3}$)	0.001	0.01	0.1	1	0.001	0.01	0.1	1
0.01	0.000	0.001	0.537	1.347	0.000	0.000	0.052	0.167
0.02	0.000	0.000	0.173	1.252	0.000	0.000	0.029	0.323
0.04	0.000	0.000	0.022	0.994	0.000	0.000	0.001	0.356
0.08	0.000	0.000	0.000	0.328	0.000	0.000	0.000	0.121

511 Note: RMSE >0.20m , >0.50m , >1.00m

512 **Table 3.** RMSE (m) error statistics for the Axisymmetric test predicted by using $\Delta t_{min} = \{100, 500,$
 513 $2000, 8000\}$ s and CellNo=50x50 ($\Delta x = 3218.7$ m) compared with the analytical solution, for four
 514 instants in time.

RMSE (m)	t (d)				
	Δt_{min}	2	3	9	12
100		0.004	0.004	0.004	0.004
500		0.004	0.004	0.005	0.005
2000		0.004	0.004	0.005	0.005
8000		0.006	0.006	0.006	0.006

515

516 **Table 4.** Efficiency statistics of the Matlab and Fortran codes for the Axisymmetric test for
 517 CellNo={300x300, 500x500, 700x700, 900x900} ($\Delta x = \{536.4, 321.9, 229.9, 178.8\}$ m) with
 518 $\Delta t_{min}=500$ s and one hour simulation time: Computational Time in seconds, Speed-up and
 519 Efficiency.

Code	Parallel Performance CellNo (Δx (m))	Computational Time (s)				Speed-up				Efficiency			
		Number of processors				Number of processors				Number of processors			
		1	2	4	12	1	2	4	12	1	2	4	12
Matlab	300x300 (536.4)	125.9	75.2	47.8	33.1	1	1.7	2.6	3.8	1	0.84	0.66	0.32
	500x500 (321.9)	348.8	196.0	120.9	75.5	1	1.8	2.9	4.6	1	0.89	0.72	0.38
	700x700 (229.9)	716.0	379.6	227.6	139.0	1	1.9	3.1	5.2	1	0.94	0.79	0.43
	900x900 (178.8)	1171.0	625.7	373.5	230.1	1	1.9	3.1	5.1	1	0.94	0.78	0.42
Fortran	300x300 (536.4)	10.7	9.4	8.8	7.3	1	1.1	1.2	1.5	1	0.57	0.30	0.12
	500x500 (321.9)	34.5	28.2	25.6	20.5	1	1.2	1.3	1.7	1	0.61	0.34	0.14
	700x700 (229.9)	66.0	56.3	52.5	39.8	1	1.2	1.3	1.7	1	0.59	0.31	0.14
	900x900 (178.8)	108.6	89.8	82.3	72.7	1	1.2	1.3	1.5	1	0.60	0.33	0.12

520

521

522

523 **A 2D Parallel Diffusive Wave Model for floodplain inundation with variable time step (P-DWave)**524 Leandro J. ^{1,3}, Chen, A. S. ², and Schumann, A. ¹

525 ¹ Institute of Hydrology, Water Management and Environmental Techniques, Ruhr-University
 526 Bochum, Germany. E-mail: Jorge.leandro@ruhr-uni-bochum.de, Andreas.Schumann@ruhr-uni-
 527 bochum.de

528 ² Centre for Water Systems, College of Engineering, Mathematics and Physical Sciences, University of
 529 Exeter, UK. E-mail: a.s.chen@exeter.ac.uk

530 ³ IMAR, Department of Civil Engineering, University of Coimbra, Portugal, R. Luís Reis Santos, Polo 2,
 531 3030-788 Coimbra, Portugal.

532 **Figure Caption**

Figure 1. Water-surface level for the “horizontal plane wetting” test predicted by P-DWave and the analytical solution (dashed line). Sensitivity analysis to the number of cells CellNo={200, 100, 50, 25} (Δx ={25, 50, 100, 200} m) with Δt_{min} ={0.001, 0.05, 0.5, 1.0} s on the front propagation.

Figure 2. Evolution of the time step solution with the iteration number (it) as a function of the number of cells discretised CellNo={200, 100, 50, 25} (Δx ={25, 50, 100, 200} m) with Δt_{min} ={0.001, 0.05, 0.5, 1.0} s during the horizontal plane wetting simulation.

Figure 3. Sensitivity analysis of the predicted water-surface level propagation to Manning’s coefficient for the “inundation of a planar beach” $S \neq 0$ test (Δx =50 m and Δt_{min} =0.001 s).

Figure 4. Evolution of the time step solution with the iteration number (it) as a function of Manning’s coefficient n ={0.01,0.02,0.04,0.08} $m^{-1/3}s$ and Δt_{min} =0.001 s during the Inundation of a planar beach $S \neq 0$ simulation.

Figure 5. Profile of the digital elevation model (DEM) (left). Water-surface levels at points 1 and 2 for the “flooding a disconnected water body” test predicted by P-Dwave and superimposed with the various models’ results published in the EA benchmark (Pender and Néelz, 2010) test for comparison (middle and right).

Figure 6. Map of the DEM showing the points locations where water levels are recorded (left). Final inundation predicted by P-Dwave (right).

Figure 7. Water-surface level for the “filling of floodplain depressions” test predicted by P-Dwave superimposed with the results from the models published in the EA benchmark (Pender and Néelz, 2010) test for comparison.

Figure 8. Map of the DEM showing the points locations where water levels are recorded (black dots) and the inflow hydrograph location (red dot) (left). Final Inundation predicted by P-Dwave overlapped with the models’s flood extents in B-EA (Pender and Néelz, 2010) (right).

533 **Figure 9.** Water-surface level for the “rainfall and point source surface flow in urban areas” test
534 predicted by P-Dwave superimposed with the results from the models published in the B-EA test
535 (Pender and Néelz, 2010).

536 **Figure 10.** Water-surface level and velocity fields ($\Delta t_{min}=100$ s) for the “Axisymmetric” test
537 predicted by the P-Dwave and the Axisymmetric model solution (dashed line) on the front
538 propagation. Sensitivity analysis of the water-surface centre profile for $\Delta t_{min}=\{100, 500, 2000,$
539 $8000\}$ s and CellNo=50x50 ($\Delta x =3218.7$ m).

Figure 11. Evolution of the time step solution with the iteration number (it) as a function of the
smallest allowable time step $\Delta t_{min}=\{100, 500, 2000, 8000\}$ s with CellNo=50x50 ($\Delta x =3218.7$ m)
during the Axisymmetric test.

540

541

542

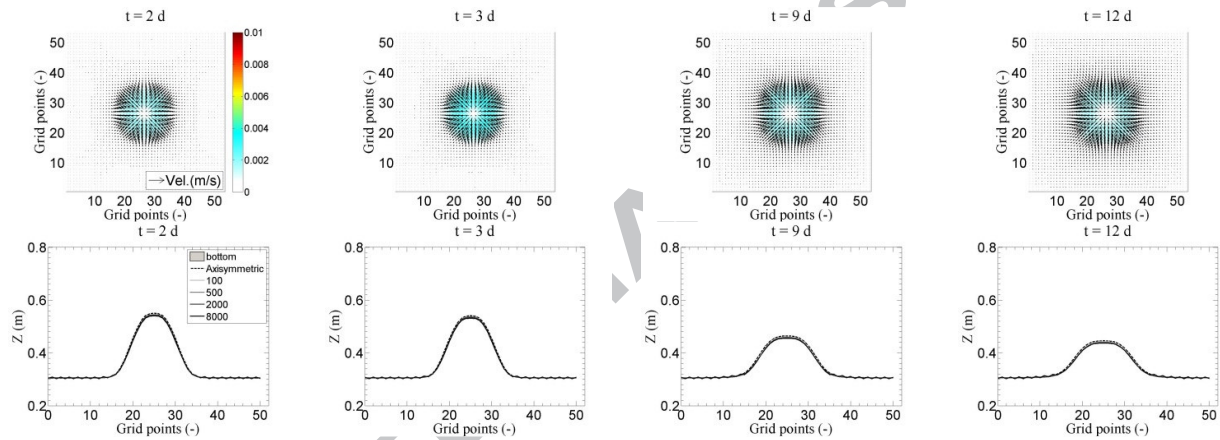
543 **A 2D Parallel Diffusive Wave Model for floodplain inundation with variable time step (P-DWave)**544 Leandro J. ^{1,3}, Chen, A. S. ², and Schumann, A. ¹545 ¹ Institute of Hydrology, Water Management and Environmental Techniques, Ruhr-University
546 Bochum, Germany. E-mail: Jorge.leandro@ruhr-uni-bochum.de, Andreas.Schumann@ruhr-uni-
547 bochum.de548 ² Centre for Water Systems, College of Engineering, Mathematics and Physical Sciences, University of
549 Exeter, UK. E-mail: a.s.chen@exeter.ac.uk550 ³ IMAR, Department of Civil Engineering, University of Coimbra, Portugal, R. Luís Reis Santos, Polo 2,
551 3030-788 Coimbra, Portugal.552 **Graphical Abstract**

Figure 10. Water-surface level and velocity fields ($\Delta t_{min}=100$ s) for the “Axisymmetric” test predicted by the P-DWave and the Axisymmetric model solution (dashed line) on the front propagation. Sensitivity analysis of the water-surface centre profile for $\Delta t_{min}=\{100, 500, 2000, 8000\}$ s and CellNo=50x50 ($\Delta x = 3218.7$ m).

553

554 **Table 4.** Efficiency statistics of the Matlab and Fortran codes for the Axisymmetric test for
555 CellNo={300x300, 500x500, 700x700, 900x900} ($\Delta x = \{536.4, 321.9, 229.9, 178.8\}$ m) with
556 $\Delta t_{min}=500$ s and one hour simulation time: Computational Time in seconds, Speed-up and
557 Efficiency.

Code	Parallel Performance CellNo (Δx (m))	Computational Time (s)				Speed-up				Efficiency			
		Number of processors				Number of processors				Number of processors			
		1	2	4	12	1	2	4	12	1	2	4	12
Matlab	300x300 (536.4)	125.9	75.2	47.8	33.1	1	1.7	2.6	3.8	1	0.84	0.66	0.32
	500x500 (321.9)	348.8	196.0	120.9	75.5	1	1.8	2.9	4.6	1	0.89	0.72	0.38
	700x700 (229.9)	716.0	379.6	227.6	139.0	1	1.9	3.1	5.2	1	0.94	0.79	0.43
	900x900 (178.8)	1171.0	625.7	373.5	230.1	1	1.9	3.1	5.1	1	0.94	0.78	0.42
Fortran	300x300 (536.4)	10.7	9.4	8.8	7.3	1	1.1	1.2	1.5	1	0.57	0.30	0.12
	500x500 (321.9)	34.5	28.2	25.6	20.5	1	1.2	1.3	1.7	1	0.61	0.34	0.14
	700x700 (229.9)	66.0	56.3	52.5	39.8	1	1.2	1.3	1.7	1	0.59	0.31	0.14
	900x900 (178.8)	108.6	89.8	82.3	72.7	1	1.2	1.3	1.5	1	0.60	0.33	0.12

558

559 **A 2D Parallel Diffusive Wave Model for floodplain inundation with variable time step (P-DWave)**560 Leandro J. ^{1,3}, Chen, A. S. ², and Schumann, A. ¹

561 ¹ Institute of Hydrology, Water Management and Environmental Techniques, Ruhr-University
562 Bochum, Germany. E-mail: Jorge.leandro@ruhr-uni-bochum.de, Andreas.Schumann@ruhr-uni-
563 bochum.de

564 ² Centre for Water Systems, College of Engineering, Mathematics and Physical Sciences, University of
565 Exeter, UK. E-mail: a.s.chen@exeter.ac.uk

566 ³ IMAR, Department of Civil Engineering , University of Coimbra ,Portugal, R. Luís Reis Santos, Polo 2,
567 3030-788 Coimbra, Portugal.

568 **Highlights**

- 569
- 570 • We develop a parallel 2D diffusive wave model in Matlab and Fortan
 - 571 • We achieved speed-up times ranging from 1.2 to 5.2 using 2 to 12 processors
 - 572 • The variable time step method and the process for Wet-dry fronts kept the solution stable
 - 573 • Absolute mass conservation is obtained in all seven tests used to validate the Model

573

574